Nonlinear Optical Properties of the Rhombic B_4-Cluster

H. REIS, M. G. PAPADOPOULOS

Institute of Organic and Pharmaceutical Chemistry, National Hellenic Research Foundation, Vasileos Constantinou 48, GR-11635 Athens, Greece

Received 18 September 1998; accepted 16 December 1998

ABSTRACT: The equilibrium geometry, energy, dipole polarizability, and second hyperpolarizability of the rhombic B_4-cluster with D_{2h} symmetry are calculated by restricted (RHF) and unrestricted (UHF) Hartree–Fock theory; Møller–Plesset perturbation theory (MPn); coupled-cluster theory with singles, doubles, and a perturbational treatment for connected triples [CCSD(T)]; Brueckner doubles with a perturbational treatment for connected triples [BD(T)]; and complete active space SCF (CASSCF) and restricted active space SCF (RASSCF) methods, using three different basis sets. The multireference methods show that excited state configurations contribute appreciably to the ground state wave function. Accordingly, the RHF method yields results that differ greatly from those of the correlated methods, even for the geometry. UHF gives more reliable geometries, but suffers from high spin contamination. The electric properties calculated at reasonably highly correlated levels are qualitatively comparable for both the single reference and multireference descriptions, although differences between CCSD(T) and BD(T) are larger than usually reported in the literature and properties calculated at the MPn ($n = 2, 3, 4$) series show much damped oscillatory behavior, especially for the components along the long in-plane axis. It is found that inclusion of *f*-functions in the basis set do not have a large effect on the electric properties. J Comput Chem 20: 679–687, 1999

Keywords: boron cluster; polarizabilities, hyperpolarizabilities

Correspondence to: M. G. Papadopoulos; e-mail: mpapad@eie.gr

Contract/grant sponsor: European Commission (TMR Network Grant); contract/grant number: ERBFMRXCT960047

CCC 0192-8651 / 99 / 070679-09

Introduction

Many experimental and theoretical studies of the energetics and structures of small homoatomic clusters have been reported over the past several years. For boron clusters, the main focus of theoretical work has been on the relationship between electronic and geometrical structures of neutral and cationic clusters[1–16] to obtain better understanding of the physical and chemical nature of boron clusters and also to explain experimentally determined cluster properties as ionization potentials and fragmentation pathways.[2] Generally, many energetically close minima on the potential surface of the electronic ground state, corresponding to different symmetries and different spin states, have been found for the small neutral B_n-clusters. For B_4, which is the subject of this work, the most stable ground state reported was generally the rhombic structure of D_{2h} symmetry with singlet spin.[2–9] Kato and Tanaka[10] reported the rhombic structure to be most stable at the MP4 level, whereas, at the SCF level, the most stable structure with a 3-21G basis set was $C_{2h}{}^3B_u$. Ray et al.,[11] employing the same basis set, found a linear structure to be more stable at the MP4 level, and the rhombic structure at the UHF and MP2 levels. However, apart from these energy/structure studies, there have been no reports about other electronic properties such as polarizabilities and hyperpolarizabilities. For some of the unique properties of boron and boron compounds, such as hardness and high-temperature resistivity, they may receive attention as candidates for nonlinear optical devices under extreme conditions. We report here the determination of linear and nonlinear properties of B_4 with D_{2h} symmetry, which is the smallest boron cluster with a singlet ground state.

The geometry has been reoptimized with different basis sets and at different levels of theory. During this work we found that the electronic ground state is not well described by a single-reference wave function at the SCF level, but that different configurations contribute appreciably and correlated methods are necessary to give a reasonable description of the properties. Therefore, we employed the multiconfigurational self-consistent field (MCSCF) method in the complete active space (CASSF) and restricted active space (RASSCF) forms and compared them with single-reference methods of different correlation orders: Many-body perturbation theory with Møller–Plesset partitioning of second to fourth order (MPn, $n = 2, 3, 4$),[17] including triple excitations for MP4 [abbreviated MP4(SDTQ)]; coupled cluster with singles, doubles, and a perturbational correction for connected triples [CCSD(T)][18]; and Brueckner doubles with a perturbational correction for triples [BD(T)].[19] Unrestricted Hartree–Fock (UHF) and MP2 (UMP2) theories were also employed. It was found that the highly correlated methods and the multireference methods yielded comparable results for the (hyper)polarizabilities, although differences, especially for components involving the long in-plane axis, remain.

Method

For geometry optimizations three basis sets were employed: the standard 6-31G*[20] basis set and the correlation-consistent polarized valence double-zeta and triple-zeta cc-pVDZ (9s5p1d) → [3s2p1d] and cc-pVTZ (10s5p2d1f) → [4s3p2d1f] basis sets developed by Dunning.[21] For the calculation of the (hyper)polarizabilities the augmented versions of these basis sets were employed, denoted 6-31 + G*,[22] aug-cc-pVDZ, and aug-cc-pVTZ,[23] where diffuse functions had been added, which are essential for the reliable calculation of (hyper)polarizabilities. Additionally, we employed the standard 6-311 + G*[22] basis set for some calculations. All single-reference calculations were performed with GAUSSIAN-94,[24] static (hyper)polarizabilities were calculated by the finite-field perturbation method of Cohen and Roothan,[25] employing an electric field value of 0.0015 a.u. It was verified that this field strength yields stable results by comparison with calculations employing higher field strengths. The Taylor expansion convention for definition of hyperpolarizabilities[26] was adopted. The MCSCF calculations used the DALTON package[27] and (hyper)polarizabilities were calculated by the response function method.[28]

The potential surface for B_4 in the SCF approximation is very flat, with the lowest normal frequency in the harmonic approximation at about 30 cm^{-1}. Therefore, very tight convergence criteria for the geometry optimization had to be applied to reach the real minima. All geometries were verified as local minima by calculating the vibrational frequencies in the harmonic approximation. Whenever possible, the Hessian was calculated analyti-

cally, except for MP4(SDTQ), CCSD(T), and BD(T), where derivatives had to be calculated numerically.

Results and Discussion

GEOMETRY

The optimized geometries, together with the energies for different methods and basis sets, are given in Table I. The coordinate system used for B_4 is shown in Figure 1.

Before discussing the geometries in detail, we must clarify the motivation for the choice of the different methods. The RHF equilibrium bond length for all three basis sets is seen to be rather short. A stability analysis of the RHF function according to ref. 29 reveals that the RHF solution is unstable with respect to an unrestricted description of the wave function, which yields an energy stabilization of 0.0117 a.u. (30.6 kJ/mol) for the cc-pVDZ basis set, at the same geometry. The other two basis sets result in similarly large energy lowerings. The optimized bond length at the UHF level is seen to be considerably larger than the RHF value and is also more in line with the results of the correlated methods. On the other hand, the UHF solution is highly spin-contaminated: the expectation value, $\langle S^2 \rangle$, where S is the total electron spin, is about 0.7 to 0.9, independent of the basis set. Spin projection of the first contaminant does not change $\langle S^2 \rangle$ considerably. A ROHF calculation of a triplet spin state yields a considerably larger energy than the RHF singlet state calculation, showing that the source of the problem is not a triplet ground state.

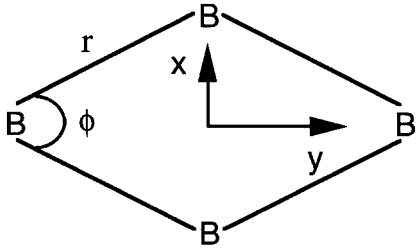

FIGURE 1. Coordinate system and geometry specification for B_4.

It has been shown that a large spin contamination of the UHF wave function is often connected with slow convergence of unrestricted Møller–Plesset perturbation theory.[30–32] This can be observed also for B_4 at the MP2 level: restricted MP2 yields a considerably lower energy than the MP2 method, based on the unrestricted wave function (cf. Table I).

Gill et al. showed that large spin contamination connected with slowly converging UMPn series may result from the presence of low-lying, doubly excited determinants, which mix with the single reference determinant.[33] In such cases, a multireference wave function can be expected to give an improved description of the electronic ground state. We performed several MCSCF calculations, employing the widely used complete active space (CASSCF) variant[34] and the restricted active space (RASSCF) variant.[35] One of the major problems in MCSCF calculations is the proper choice of the active space of occupied and virtual orbitals. Jensen et al. proposed to choose the active space according to the occupation numbers of the natural orbitals (NO) resulting from a previous MP2 calcula-

TABLE I.
Optimized Geometry Parameters and Energies Calculated with Different Correlated and Uncorrelated Methods and Basis Sets.

	6-31G*			cc-pVDZ			cc-pVTZ		
Method	r/Å	ϕ/deg.	E/a.u.	r/Å	ϕ/deg.	E/a.u.	r/Å	ϕ/deg.	E/a.u.
RHF	1.509	85.0	−98.4240	1.520	90.0	−98.4382	1.506	90.0	−98.4597
UHF	1.551	90.0	−98.4398	1.561	90.0	−98.4529	1.544	90.0	−98.4709
UMP2	1.532	82.0	−98.7383	1.563	90.0	−98.7400			
MP2	1.551	73.1	−98.7636	1.576	73.6	−98.7646	1.546	74.1	−98.8423
MP4	1.563	71.8	−98.8106	1.588	72.3	−98.8114	1.557	72.9	−98.8898
CAS1	1.564	67.2	−98.4564	1.572	67.8	−98.4682			
CAS2	1.548	73.2	−98.5635	1.557	73.9	−98.5744			
RAS	1.554	73.0	−98.6686	1.565	73.8	−98.6794	1.546	73.6	−98.7019
BD(T)	1.551	74.5	−98.8069	1.575	75.8	−98.8081			

tion.[36] They also showed that using the natural orbitals of the MP2 calculation as an initial guess, greatly improves the convergence behavior of the subsequent CASSCF calculations. The occupation numbers of the natural orbitals with occupation numbers larger than 0.001 calculated with the aug-cc-pVDZ basis sets are shown in Table II. The four core orbitals were not correlated and are doubly occupied. In general, the results do not depend considerably on the basis set and geometry employed. All strongly occupied valence orbitals have occupation numbers significantly lower than 2. Similarly, a large number of weakly occupied orbitals are significantly occupied. An active space involving all the relevant orbitals would have been prohibitively large, therefore we choose different subsets. The simplest active space chosen consists of two electrons, distributed over two orbitals—the one strongly occupied with the lowest occupation number in the MP2-NO ($2a_g$) and the weakly occupied orbital with the highest occupation number ($2b_{2u}$). This two-configuration wave function is abbreviated by CAS1 and resembles a two-configuration generalized valence bond (GVB) function,[37] a method that is also used for the description of static degeneracy problems.[38] The contributions of the SCF configuration $|\ldots 2a_g^2|$ and the excited configuration $|\ldots 2b_{2u}^2|$ in the final CAS1 wave function were 83.5% and 16.5%, respectively, showing that the admixture of excited configurations into the ground-state wave function is in fact considerable.

In a second active space, denoted by CAS2, ten electrons were distributed over ten orbitals ($2-3a_g, 1-2b_{3u}, 1-2b_{2u}, 1b_{1g}, 1b_{1u}, 1b_{3g}, 1b_{2g}$). This choice generated 2540 configurational-state functions. Here, the SCF configuration retained a contribution of 80.8% and the excited configuration with $2b_{2u}^2$ instead of $2a_g^2$ still had the largest weight of the excited configurations in the final CAS2 wave function, but its contribution dropped to 2.9%, followed in magnitude by the configuration with the replacement $2a_g^2 \rightarrow 3a_g^2$ with a contribution of 1.8% and three other configurations with contributions of more than 1% and a further six configurations with contributions between 0.5% and 1%. This shows that, in fact, a larger number of excited configurations contribute to the ground-state wave functions with similar weights and that the two-configuration description is probably inadequate.

Finally, we employed a restricted active space calculation, which is an extension of the CASSCF method, where the active space is divided into three subspaces: RAS1 consists of strongly occupied orbitals, from which only a limited number of electrons are allowed to be removed; RAS2 is an analog to CAS, where the electrons in strongly occupied orbitals are distributed in all possible ways among the weakly occupied orbitals; and RAS3 consists of a number of weakly occupied orbitals to which only a limited number of electrons may be excited. By including a limited CI in an optimized orbital space, RASSCF calculations can recover a part of the dynamic correlation in addition to the nondynamical correlation taken into account by the RAS2 space.[39] In our case, RAS1 consisted of four orbitals ($1a_g, 1b_{3u}, 1b_{2u}, 1b_{1g}$), RAS2 comprised six orbitals ($2-3a_g, 2b_{3u}, 2b_{2u}, 1b_{1u}, 1b_{3g}, 1b_{2g}$), and RAS3 consisted of another six orbitals ($4-5a_g, 3b_{3u}, 3b_{2u}, 2b_{1g}, 2b_{1u}$). Four electrons were distributed in RAS2, up to two electrons were excited from RAS1, and all single and double excitations were allowed for RAS3. A total of 29,712 configurations were created in this way. The SCF configuration contributed 78.6% to the RAS wave function; the main contributing excited configurations were generally the same as in the CAS2 function, and their weights were also similar.

Single-reference methods including electron correlation effects may also provide an adequate de-

TABLE II.
Occupation Numbers (> 0.001) of MP2 Natural Orbitals (Core Orbitals Doubly Occupied).

a_g	b_{3u}	b_{2u}	b_{1g}	b_{1u}	b_{3g}	b_{2g}	a_u
1.9772							
1.8748	1.9438	1.9474	1.9342	1.8921			
0.0535	0.0402	0.0825	0.0154	0.0145	0.0398	0.0573	0.0068
0.0168	0.0213	0.0179	0.0083	0.0078	0.0021	0.0025	
0.0112	0.0044	0.0035			0.0013	0.0013	
0.0044	0.0014	0.0027					
0.0012	0.0011	0.0015					

scription of the electronic ground state of molecules for which the SCF description is inadequate, provided the order of correlation treatment is high enough.[40,41] We employed, for geometry optimization, the popular MPn perturbation methods and, as a more accurate method, the Brueckner doubles with perturbation treatment for triples [BD(T)].

Table I shows that the optimized geometries at the uncorrelated levels correspond to a square (D_{4h} symmetry), except for RHF/6-31G*. This is in contrast to the higher correlated levels, which generally yield a rhombic structure with D_{2h} symmetry, except for UMP2 with the cc-pVDZ basis set with a square geometry. As mentioned earlier, the geometry convergence criteria applied had to be very tight to obtain these results; otherwise, the optimization process would get stuck on a part of the potential surface of small gradients, corresponding to a structure of D_{2h} symmetry, but not corresponding to a minimum. In general, the single-reference correlation methods and the MCSCF methods yield comparable results for the geometry, except for CAS1, which gives a rather exaggerated rhombic structure.

Dynamic correlation effects tend to lengthen the bond length, as can be seen by comparing the CAS2 results with those of the other correlation methods. There is no similar effect on the bond angles.

Comparing the different basis sets, it can be seen that the cc-pVDZ basis set gives significantly larger bond lengths than the other two basis sets, with the bond lengths for cc-pVTZ being slightly shorter than those for 6-31G*. To assess which is the more adequate basis set, we performed geometry optimizations at the UHF, UMP2, and UMP4 levels on the triplet ground state of B_2, for which an experimental bond length value of 1.59 Å has been found.[42] The results given in Table III show that both 6-31G* and cc-pVTZ basis sets reproduce the bond length accurately at the correlated levels, whereas the cc-pVDZ basis overestimates the bond length considerably. We therefore take the data calculated at the BD(T) level with the 6-31G* basis set as the best estimate for the geometry of B_4.

Our results for the geometry and the energy of B_4 for the 6-31G* basis set compare very well with those of Martin et al.[6] at the RHF level, whereas, at the MP2 level, our bond length is 0.004 Å larger than that reported by Martin et al. The reason for this discrepancy is unclear. Generally, the bond lengths of rhombic B_4 reported in the literature are smaller than those reported here: 1.51 Å for 3-21G/MP4[11]; 1.528 Å for a van Dujneveldt-type basis set (9s, 4p) → [4s, 2p] at the RHF level[43]; 1.516 Å for a double-zeta plus polarization function at the HF(AE)-CI level[4]; and 1.51 Å for a (10s, 5p, 1d) → [3s, 2p, 1d] basis set at the MP4(SDTQ) level.[8]

POLARIZABILITIES AND HYPERPOLARIZABILITIES

The polarizabilities and second hyperpolarizabilities of B_4 calculated at different levels of theory, geometries, and basis sets are given in the Tables IV–VII. In Table IV, the properties calculated at the geometries optimized at the respective level and basis set without diffuse functions are shown, except for the CCSD(T) level, where the CAS2-optimized geometry was used. The results for UHF and UMP2 are not shown, because they gave very large negative values for γ_{xxxx} and γ_{yyyy}, and were considered to be physically unreasonable, considering their large spin contamination. Both for the polarizability and for the second hyperpolarizability the values of the diagonal components in the long in-plane axis are the components most sensitive regarding the model and basis set employed. The Hartree–Fock and CAS1

TABLE III.
Optimized Bond Lengths and Energies of B_2 for Different Basis Sets.

	6-31G*		cc-pVDZ		cc-pVTZ	
Method	r/Å	E/a.u.	r/Å	E/a.u.	r/Å	E/a.u.
UHF	1.635	−49.0753	1.650	−49.0871	1.638	−49.0926
UMP2	1.596	−49.2177	1.621	−49.2261	1.599	−49.2529
UMP4	1.600	−49.2575	1.632	−49.2671	1.606	−49.2921
Exp.[42]	r = 1.59 Å					

TABLE IV.
Polarizabilities (α) (a.u.) and Second Hyperpolarizabilities γ (a.u.) of B_4 Calculated at Optimized Geometries at the Same Levels and Basis Sets without Diffuse Functions.

Method	α_{xx}	α_{yy}	α_{zz}	α_{av}[a]	γ_{xxxx}	γ_{yyyy}	γ_{zzzz}	γ_{xxyy}	γ_{yyzz}	γ_{xxzz}	γ_{av}[b]
6-31 + G*											
RHF	63.0	95.3	37.4	65.2	45000	77500	18100	15400	16800	10200	45100
MP2	55.3	73.7	35.5	54.9	27500	73000	14400	11900	6900	6600	33100
MP4	55.7	76.6	35.0	55.8	24000	59700	14500	10200	7300	6400	29200
CAS1	57.5	84.3	39.2	60.3	16200	143800	15700	7600	6300	4800	42700
CAS2	58.0	83.5	34.0	58.5	19500	38900	12500	9500	5700	8700	23700
RAS	53.9	82.9	34.4	57.1	19800	39900	14000	9700	6100	9000	24700
aug-cc-pVDZ											
RHF	74.5	74.5	41.4	63.5	54400	54400	13700	10800	11400	11400	38000
MP2	58.2	75.0	40.6	57.9	19900	67500	11000	9900	6000	6200	28500
MP4	58.5	78.9	40.4	59.3	17800	54300	10600	8100	5500	6400	25000
CCSD(T)[c]	57.4	84.2	39.7	60.4	21800	47400	10800	9800	6100	9000	26000
BD(T)	59.3	84.2	40.4	61.3	23000	40900	11200	10100	6400	9000	25200
CAS1	58.2	85.9	43.4	74.4	12100	138000	11900	6200	5300	4200	38700
CAS2	56.0	83.7	38.5	59.4	16100	32000	9000	7900	4800	7500	19500
RAS	55.3	83.6	39.2	59.4	16000	34300	8800	8000	5400	7700	20100
aug-cc-pVTZ											
RHF	72.8	72.8	40.4	62.0	52300	52300	16400	11900	10900	10900	37700
MP2	56.1	75.0	39.2	56.7	19600	49000	11800	9900	5700	6600	25000

[a] $\alpha_{av} = 1/3(\alpha_{xx} + \alpha_{yy} + \alpha_{zz})$. [b] $\gamma_{av} = 1/5(\gamma_{xxxx} + \gamma_{yyyy} + \gamma_{zzzz} + 2(\gamma_{xxyy} + \gamma_{xxzz} + \gamma_{yyzz}))$. [c] CAS2/cc-pVDZ-optimized geometry.

TABLE V.
Model Dependence of Polarizability (α) and Second Hyperpolarizability (γ) of B_4 Calculated with aug-cc-pVDZ Basis Set at BD(T) / 6-31G*-Optimized Geometry.

Method	α_{xx}	α_{yy}	α_{zz}	α_{av}	γ_{xxxx}	γ_{yyyy}	γ_{zzzz}	γ_{xxyy}	γ_{yyzz}	γ_{xxzz}	γ_{av}
RHF	61.1	105.2	42.1	69.5	32400	66300	14900	14900	8900	15600	38100
MP2	57.0	76.1	39.7	57.6	20200	49200	10800	9900	6000	7100	25300
MP3	56.4	84.0	39.5	60.0	16300	17800	9800	9800	5000	6800	17400
MP4	56.9	77.9	39.2	58.0	18000	42700	10000	8500	5400	6900	22500
CCSD(T)	57.3	83.2	39.5	60.0	22100	46000	10800	9700	6200	9000	25700
BD(T)	57.2	83.5	39.5	60.1	21000	39100	10700	9900	6000	8700	24000
CAS2	56.1	83.6	38.5	59.4	16300	32000	9100	7900	4800	7500	19600

TABLE VI.
Polarizabilities (α) and Second Hyperpolarizabilities (γ) (a.u.) of B_4 Calculated at the RHF and MP*n* Levels with aug-cc-pVDZ Basis Set at MP4 / cc-pVDZ-Optimized Geometry.

Method	α_{xx}	α_{yy}	α_{zz}	α_{av}	γ_{xxxx}	γ_{yyyy}	γ_{zzzz}	γ_{xxyy}	γ_{yyzz}	γ_{xxzz}	γ_{av}
RHF	62.2	116.7	43.7	74.2	31500	64000	15800	16000	9100	17800	39400
MP2	58.5	73.1	41.0	57.5	19400	96800	11500	9500	6300	5500	34100
MP3	57.7	87.0	40.9	61.9	15700	24900	10500	10500	5200	6000	18900
MP4	58.5	78.9	40.4	59.3	17800	54300	10600	8100	5500	6400	24500

TABLE VII.
Basis Set Dependence of Polarizability (α) and Second Hyperpolarizability (γ) of B_4 Calculated at MP2 and CAS2 Levels Using the Respective 6-31G*-Optimized Geometries.

Basis set	α_{xx}	α_{yy}	α_{zz}	α_{av}	γ_{xxxx}	γ_{yyyy}	γ_{zzzz}	γ_{xxyy}	γ_{yyzz}	γ_{xxzz}	γ_{av}
MP2											
6-31 + G*	55.3	73.7	35.5	54.9	27500	7300)	14400	11900	6900	6600	33100
6-311 + G*	55.3	74.2	35.2	54.9	18600	62000	13500	8400	4900	4800	26100
aug-cc-pVDZ	56.5	75.6	39.7	57.3	19200	60800	10700	9500	5800	6700	26900
aug-cc-pVTZ	55.9	74.5	39.3	56.6	18900	59900	11900	9500	5600	6200	26700
CAS2											
6-31 + G*	58.0	83.5	34.0	58.5	19500	38900	12500	9500	5700	8700	23700
6-311 + G*	56.2	82.7	34.5	57.8	16200	31600	12300	7500	4600	6700	19500
aug-cc-pVDZ	56.3	82.6	38.4	59.1	16800	31600	9000	7900	4900	7400	19600
aug-cc-pVTZ	56.3	82.7	38.2	59.1	17900	32400	11000	8800	5100	7600	20900

values differ largely from those of the other models, which is not surprising considering the shortcomings of the two models already discussed. CAS1 gives especially large values for γ_{yyyy}, similarly as it exaggerates the extension of the cluster in the *y*-direction. This suggests an improperly balanced description of the two-configuration wave function for the electronic ground state. Comparing the two more-balanced MCSCF descriptions, CAS2 and RAS, it can be seen that they give very similar results for the electronic properties, with no more than 10% difference in the single components.

To get a clearer picture of the model dependence of the electronic properties, we calculated them for a variety of models employing one basis set (aug-cc-pVDZ) and the same geometry. The results are shown in Table V, which also includes a calculation at the MP3 level. The MP*n* series shows a strong oscillatory behavior, especially regarding in-plane components of the second hyperpolarizability. But, not all components are oscillating: α_{zz} and γ_{xxyy} are merely monotonically decreasing. A similar oscillating behavior has been reported elsewhere (e.g., for the dipole moment, polarizability, and quadrupole moment components of ozone).[41] Comparison of the results for MP4(SDTQ) with the higher order methods CCSD(T) and BD(T) shows that the latter generally give higher values for the different components than MP4(SDT), except for γ_{yyyy} in the case of BD(T), which is about 2.9% lower than the value for MP4(SDTQ). If the oscillatory behavior of the MP*n* series will finally yield converged values for the electric properties, the converged results should lie between the MP3 and the MP4 values. Most of the values of the higher order methods lie outside this range. This may indicate either that the perturbational order of BD(T) and CCSD(T) is still not high enough to give highly accurate values or that the MP*n* series does not converge at all, as is known to occur in multiconfigurationally dominated systems and also shown to occur in the case of single-configuration-dominated systems.[44] On the other hand, with an eye to more qualitative agreement, the different higher order methods yield surprisingly similar results, including CAS2, which gives the values that differ by at most 30% from those of BD(T). It is also of interest to note that the γ_{yyyy} component differs by as much as 20% between CCSD(T) and BD(T). In other cases, both methods give very similar results for the (hyper)polarizabilities, as has been shown by Kobayashi et al. for several small molecules.[45]

In Table VI the values of the properties for the MP*n* series calculated at a geometry with a larger bond length and a slightly more rhombic structure are shown. The oscillation for γ_{yyyy} is now increased considerably, the γ_{xxyy} component shows a rather erratic behavior, and γ_{yyzz} is monotonically *increasing*. This shows a surprising *geometric dependence of the oscillatory behavior* of the second hyperpolarizability for the MP*n* series, although the actual geometry changes are not very large ($\Delta r = 0.037$ Å, $\Delta\phi = 2.2°$). This may be another indication for divergent behavior of the MP*n* series.

The dependence of the (hyper)polarizabilities from the basis set employed can be seen in Table VII for CAS2 and MP2, calculated at the respective 6-31G*-optimized geometry. We included the 6-311 + G* basis, which was optimized at the correlated MP2 level.[22] For both methods, the polariz-

ability components, α_{xx} and α_{yy}, are nearly the same for all basis sets, whereas α_{zz} is about 10% lower for the 6-31x + G* basis sets. The Dunning aug-cc-pVXZ basis sets have more diffuse functions than the 6-31x + G* basis sets. Therefore, diffuse functions seem to be more important for α_{zz} than for the other components. For γ, the differences between the two 6-31x + G* basis sets are larger, with the 6-311 + G* values generally lower than the 6-31 + G* values; however, the values are nearly the same for the aug-cc-pVDZ and aug-cc-pVTZ basis sets, indicating that the aug-cc-pVDZ basis is already a complete set for γ and *f*-functions are not important. The patterns for the two methods, CAS2 and MP2, are very similar, indicating that the same conclusions may also hold for the higher order methods.

Synopsis

In general, the electric properties α and γ of B_4 calculated at correlated levels are qualitatively similar, if taken to sufficiently high order. The single-reference RHF approach overestimates the properties considerably, as does the two-configuration description CAS1, although to a lesser extent. Similarly, the geometries from both methods differ largely from those of the other methods; that is, whereas the RHF method tends to give square geometries, CAS1 yields exaggerated rhombic structures. The UHF and UMP2 methods result in unphysically large and negative electric properties, probably due to large spin contamination. The more sophisticated methods, MP4, CCSD(T), BD(T), CAS2, and RAS, however, yield values for α_{av} and γ_{av} differing by less than 4% and 25%, respectively, although the discrepancies, especially for the components in the long in-plane axis, are somewhat higher.

Considering the fact that the aug-cc-pVDZ basis set is already an essentially saturated set for the description of the electric properties, we believe that our best values give a good estimate for the electronic contribution to the static values of B_4, which we estimate to fall in the range of values $\alpha_{av} = 60 \pm 2$ a.u. and $\gamma_{av} = 23{,}000 \pm 4000$.

References

1. Boustani, I. Int J Quantum Chem 1994, 52, 1081.
2. Hanley, L.; Whitten, J. L.; Anderson, S. L. J Phys Chem 1988, 92, 5803.
3. Boustani, I. Private communication.
4. Bonačić-Koutecký, V.; Fantucci, P.; Koutecký, J. Chem Rev 1991, 91, 1035.
5. Kato, H.; Yamashita, K. Chem Phys Lett 1992, 190, 361.
6. Martin, J. M. L.; François, J. P.; Gijbels, R. Chem Phys Lett 1992, 189, 529.
7. Koutecký, J.; Pacchioni, G.; Jeung, G. H.; Hass, E. C. Surf Sci 1985, 156, 651.
8. Niu, J.; Rao, B. K.; Jena, P. J Chem Phys 1997, 107, 132.
9. Whiteside, R. A. PhD thesis; Carnegie-Mellon University, Pittsburgh, PA, 1981.
10. Kato, H.; Tanaka, E. J Comput Chem 1991, 12, 1097.
11. Ray, A. K.; Howard, I. A.; Kanal, K. M. Phys Rev B 1992, 45, 14247.
12. Boustani, I. Chem Phys Lett 1995, 240, 135.
13. Boustani, I. Chem Phys Lett 1995, 233, 273.
14. Hernandez, R.; Simons, J. J Chem Phys 1991, 94, 2961.
15. Ricca, A.; Bauschlicher, C. W., Jr. Chem Phys 1996, 208, 233.
16. Tang, A.-C.; Li, Q.-S.; Liu, C.-W.; Li, J. Chem Phys Lett 1993, 201, 465.
17. Møller, C.; Plesset, M. S. Phys Rev 1934, 46, 618; Pople, J. A.; Binkley, J. S.; Seeger, R. Int J Quantum Chem Symp 1976, 10, 1; Pople, J. A.; Krishnan, R.; Schlegel, H. B.; Binkley, J. S. Int J Quantum Chem Symp 1978, 14, 545; Krishnan, R.; Frisch, M. J.; Pople, J. A. J Chem Phys 1980, 72, 4244.
18. Coester, F. Nucl Phys 1958, 7, 421; Coester, F.; Kümmel, H. Nucl Phys 1960, 17, 477; Čižek, J. J Chem Phys 1966, 45, 4256.
19. Brueckner, K. A. Phys Rev 1954, 96, 508; Chiles, R. A.; Dykstra, C. E. J Chem Phys 1981, 74, 4544; Handy, N. C.; Pople, J. A.; Head-Gordon, M.; Raghavachari, K.; Trucks, G. W. Chem Phys Lett 1989, 164, 185.
20. Hariharan, P. C.; Pople, J. A. Chem Phys Lett 1972, 66, 217.
21. Dunning, T. H., Jr. J Chem Phys 1988, 90, 1007.
22. Clark, T.; Chandrasekar, J.; Spitznagel, G. W.; von R. Schleyer, P. J Comput Chem 1983, 4, 294.
23. Kendall, R. A.; Dunning, T. H., Jr.; Harrison, R. J. J Chem Phys 1992, 96, 6796.
24. Frisch, M. J.; Trucks, G. W.; Schlegel, H. B.; Gill, P. M. W.; Johnson, B. G.; Robb, M. A.; Cheeseman, J. R.; Keith, T.; Petersson, G. A.; Montgomery, J. A.; Raghavachari, K.; Al-Laham, M. A.; Zakrzewski, V. G.; Ortiz, J. V.; Foresman, J. B.; Cioslowski, J.; Stefanov, B. B.; Nanayakkara, A.; Challacombe, M.; Peng, C. Y.; Ayala, P. Y.; Chen, W.; Wong, M. W.; Andres, J. L.; Replogle, E. S.; Gomperts, R.; Martin, R. L.; Fox, D. J.; Binkley, J. S.; Defrees, D. J.; Baker, J.; Stewart, J. P.; Head-Gordon, M.; Gonzalez, C.; Pople, J. A. GAUSSIAN-94, Rev D.4; Gaussian: Pittsburgh, PA, 1995.
25. Cohen, H. D.; Roothaan, C. C. J. J Chem Phys 1965, 43, S34.
26. Willets, A.; Rice, J. E.; Burland, D. M.; Shelton, D. P. J Chem Phys 1992, 97, 7590.
27. Helgaker, T.; Jensen, H. J. A.; Jørgensen, P.; Olsen, J.; Ruud, K.; Ågren, H.; Andersen, T.; Bak, K. L.; Bakken, V.; Christiansen, O.; Dahle, P.; Dalskov, E. K.; Enevoldsen, T.; Fernandez, B.; Heiberg, H.; Hettema, H.; Jonsson, D.; Kirkepar, S.; Kobayashi, R.; Koch, H.; Mikkelsen, K. V.; Norman, P.;

Packer, M. J.; Saue, T.; Taylor, P. R.; Vahtras, O. DALTON, Release 1.0, 1997.

28. Olsen, J.; Jørgensen, P. J Chem Phys 1985, 82, 3235; Jørgensen, P.; Jensen, H. J. A.; Olsen, J. J Chem Phys 1988, 89, 3654; Jonsson, D.; Norman, P.; Ågren, H. J Chem Phys 1996, 105, 6401.
29. Seeger, R.; Pople, J. A. J Chem Phys 1977, 66, 3045.
30. Knowles, P. J.; Somasundram, K.; Handy, N. C.; Hirao, K. Chem Phys Lett 1985, 113, 8.
31. Nobes, R. H.; Pople, J. A.; Radom, L.; Handy, N. C.; Knowles, P. J. Chem Phys Lett 1987, 138, 481.
32. Gill, P. M. W.; Pople, J. A.; Radom, L.; Nobes, R. H. J Chem Phys 1988, 89, 7307.
33. Gill, P. M. W.; Radom, L. Chem Phys Lett 1986, 132, 16.
34. Malmqvist, P.-Å.; Rendell, A.; Roos, B. O. Chem Phys 1990, 94, 5477.
35. Olsen, J.; Roos, B. O.; Jørgensen, P.; Jensen, H. J. A. J Chem Phys 1985, 89, 2185.
36. Jørgen, H.; Jensen, A.; Jørgensen, P. J Chem Phys 1988, 88, 3834.
37. Roos, B. O. Adv Chem Phys 1987, LXLX, 399.
38. Goddard, W. A., III; Dunning, T. H., Jr.; Hunt, W. J.; Hay, P. J. Acc Chem Res 1973, 6, 368.
39. Luo, Y.; Ågren, H. Adv Quantum Chem 1995, 26, 165.
40. Stanton, J. F.; Lipscomb, W. N.; Magers, D. H.; Bartlett, R. J. J Chem Phys 1989, 90, 1077.
41. Andersson, K.; Borowski, P.; Fowler, P. W.; Malmqvist, P.-Å.; Roos, B. O.; Sadlej, A. J. Chem Phys Lett 1992, 190, 367.
42. Douglas, A. E.; Herzberg, G. Can J Res Sect A 1940, 18, 165.
43. Boustani, I. Phys Rev B 1997, 55, 16426.
44. Christiansen, O.; Olsen, J.; Jørgensen, P.; Koch, H.; Malmqvist, P.-Å. J Chem Phys 1996, 261, 369.
45. Kobayashi, R.; Koch, H.; Jørgensen, P.; Lee, T. J. Chem Phys Lett 1993, 211, 94.